Speckle correlation measurement in a disordered medium observed through second-harmonics generation

Tetsu Ito and Makoto Tomita
Department of Physics, Faculty of Science, Shizuoka University, 836 Ohya, Shizuoka 422-8529, Japan
(Received 8 November 2002; revised manuscript received 7 October 2003; published 31 March 2004)

We examined speckle correlation in a disordered medium consisting of $LiNbO_3$ corpuscles, by observing the total intensity of the second-harmonics (SH) light generated by angular correlated two excitation beams. The total SH intensity showed a correlation peak at $\theta \sim 0$, where θ was the angle between two excitation beams, and decreased as θ was increased. The observation could be understood as the effect of the constructive interference between two volume speckle patterns produced by the excitation beams inside the medium, and the peak could reflect the mutual correlation between two patterns. The experimental results showed good agreements with a theoretical analysis based on a diffusion approximation.

DOI: 10.1103/PhysRevE.69.036610 PACS number(s): 42.25.Dd, 42.30.Ms, 42.65.−k, 42.62.Fi

I. INTRODUCTION

Localization and fluctuations are fundamental problems in wave propagation in disordered media [1]. Various effects on the coherent backscattering peak have been examined in order to clarify the nature of weak localization of photon [2–8]. A microlaser consisting of semiconductor powders was reported and the sharp structures in the emission spectrum were discussed on the basis of coherent feed back due to recurrent scattering loops [9–11]. On the other hand, when a coherent wave propagates through a disordered medium, large intensity fluctuations appear owing to the random interference effect among multiply scattered waves. Such intensity fluctuations are referred to as speckle [12]. It was shown that the coherent backscattering peak reveals its profile, only after speckle fluctuations are ensembled averaged over many possible random configurations of the sample [4,5]. Various kinds of correlations in speckle fluctuations have been investigated [13–19]. The long and infinite range correlations are the higher order correlations [15–18], which are relevant to the universal conductance fluctuations in a mesoscopic electric system [20]. The effect of absorption on the correlations [21] and the time resolved effect have also been investigated [22,23]. It should be noted that in all experiments so far reported, speckle was examined essentially using a single laser beam. That is, a single incoming laser beam is irradiated onto the disordered medium and a reference speckle pattern is recorded using a photomultiplier tube or a charge coupled device camera. Then, another fluctuation pattern is reordered again after the experimental condition is changed. The mutual correlation between two speckle patterns is numerically calculated in a computer.

Nonlinear optical phenomena have also been attracting much interest in disordered media [7,19,24–28]. In a previous paper, we used a two beam correlation method to investigate the gain volume in an amplifying and scattering medium [29,30]. In this method, two excitation beams were injected onto the sample, and the spectral width of the emission light, as the nonlinear optical signal, was monitored as a function of the spatial separation distance between the two excitation beams. In the above experiment, only beam intensity was utilized to measure the diffusion process of the excited region. However, if we utilize the wave nature of the incident beams, the two beam correlation method could also be used potentially to examine fluctuations and the correlation effects [31].

The concept is schematically illustrated in Fig. 1(a). In contrast to the traditional speckle measurements, two laser beams are injected simultaneously on the sample. Then, the second-harmonics (SH) light generated inside the medium is collected and the total SH intensity is monitored as a function of the angle between two beams. Note that no real pattern of the speckle fluctuations is monitored. When two beams have the same wave vector, wavelength, and polarization, speckle pattern produced by each beam is identical with respect to each other. In this situation, two speckle patterns should interfere constructively, and generate the enhanced SH intensity. On the other hand, when the wave vector of the second beam is slightly changed, the speckle pattern produced by this second beam changes gradually. Therefore, we

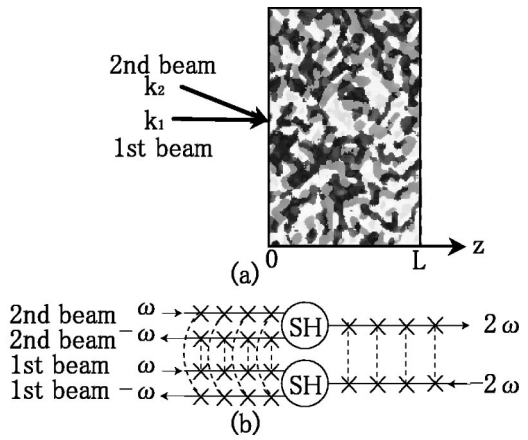

FIG. 1. (a) Schematic illustration of the volume speckle patterns inside the medium produced by two excitation beams. Black and gray patterns represent speckle patterns produced by the first and second beams, respectively. (b) Feynman diagram for $C(\Delta k)$ represented by Eq. (5). The solid lines denote the ensemble averaged Green function and dotted lines represent the ensemble averaged scattering in the medium.

could directly obtain the correlation of the speckle fluctuations inside the medium by measuring the total SH intensity from the medium as a function of angle θ between two excitation beams.

II. THEORY

We theoretically describe the SH generation in the nonlinear disordered medium. Two excitation beams with wave vectors k_1 and k_2 are injected onto the medium as shown in Fig. 1 (a). The excitation light propagates in the medium and appears as a local electric field. The local electric field at position r_s inside the medium is represented as the sum of electric fields propagated through all possible trajectories,

$$E_{local}(r_s) = \int dR \sum_{i=1,2} E_i(R) \exp[ik_i R] \sum_{\xi=all} W_\xi(r_s;R), \tag{1}$$

where R is the transverse vector in the incoming surface of the sample and $E_i(R)$ is the electric field of ith ($i=1$ or 2) excitation beam. $P=|W_\xi(r_s;R)|^2$ is the probability that the intensity propagates from R to r_s along a trajectory ξ. The total SH intensity may be described on the basis of the intensity correlation of the excitation light at r_s as

$$I_{SH}(\Delta k) = \int dR_d \int dr_s C(r_s,\Delta k) T_{SH}(R_d;r_s), \tag{2}$$

where

$$\begin{aligned} C(r_s,\Delta k) = \eta \int dR_1 \int dR_2 \int dR_3 \int dR_4 \\ \times \sum_{i,j,k,l=1,2} E_i(R_1) E_j^*(R_2) E_k(R_3) E_l^*(R_4) \\ \times \exp[i(k_i R_1 - k_j R_2 + k_k R_3 - k_l R_4)] \\ \times \left\langle \sum W_{\xi_1}(r_s;R_1) W_{\xi_2}^*(r_s;R_2) W_{\xi_3}(r_s;R_3) \right. \\ \left. \times W_{\xi_4}^*(r_s;R_4) \right\rangle \end{aligned} \tag{3}$$

is the intensity correlation of the local excitation intensity at point r_s and η is a proportional factor for the SH generation. The notation $T_{SH}(R_d;r_s)$ represents the intensity propagator for the SH light from r_s inside the medium to the detection point R_d on the boundary of the sample. The four probability amplitudes in Eq. (3) are random Gaussian variables. We have two types of terms for which the ensemble average does not vanish [32]:

$$\begin{aligned} \left\langle \sum_{\xi_1,\xi_2,\xi_3,\xi_4=all} W_{\xi_1}(R_1) W_{\xi_2}^*(R_2) W_{\xi_3}(R_3) W_{\xi_4}^*(R_4) \right\rangle \\ = \left\langle \sum |W_{\xi_1}(R_1)|^2 \right\rangle \left\langle \sum |W_{\xi_3}(R_3)|^2 \right\rangle \delta(R_1-R_2) \\ \times \delta(R_3-R_4) + \left\langle \sum |W_{\xi_1}(R_1)|^2 \right\rangle \left\langle \sum |W_{\xi_3}(R_3)|^2 \right\rangle \\ \times \delta(R_1-R_4)\delta(R_3-R_2), \end{aligned} \tag{4}$$

where we introduced a shortened notation, $W_\xi(r_s,R) \equiv W_\xi(R)$. In the present situation of the SH generation, it is not necessary to distinguish the two terms on the right-hand side of Eq. (4), since these terms are degenerated when the suffix order of the electric fields is replaced. We will consider the first term below, but the second term can be treated in the same manner. Four electric fields in Eq. (3) $E(R)$ are provided by either the first or the second beam, therefore we have a total of $2^4=16$ ways to make the four-field combination. Eight of the 16 terms, where one of the four electric fields of i,j,k and l is either 1 or 2 and the other three fields are 2 or 1 accordingly, are oscillating terms by $\cos[\Delta\phi]$ as a function of the relative phase of the first and second beams $\Delta\phi$. The two terms, where $i=k=1$, $j=l=2$ and $i=k=2$, $j=l=1$, are oscillating by $\cos[2\Delta\phi]$. Four terms, that is, $i=j=1$, $k=l=2$ term, $i=j=2$, $k=l=1$ term, and $i=j=k=l=1$ or 2 terms, are base terms, and are independent of $\Delta k=k_1-k_2$. The remaining two terms, that is, $i=l=1$, $k=j=2$, term and $i=l=2$, $k=j=1$ term, present the Δk correlation of speckles in the medium. The intensity correlation that contributes to the angular correlation of speckle fluctuations in Eq. (3) is written as

$$\begin{aligned} C(r_s,\Delta k) = \left| \int dR E_1(R) E_2^*(R) \exp[i\Delta k R] \right. \\ \left. \times \left\langle \sum |W_\xi(r_s;R)|^2 \right\rangle \right|^2. \end{aligned} \tag{5}$$

The Feynman diagram which represents this term is illustrated in Fig. 1(b).

We consider a slab geometry as an example and calculate the correlation function of Eq. (5) on the basis of the diffusion approximation. We assume that the sample exists $0 \leqslant z \leqslant L$ region and the z axis is taken to be perpendicular to the incoming surface. In the use of the diffusion approximation, the effect of the internal reflection at the boundary of disordered medium is very important, specifically in the reflection geometry. This effect could be quantitatively treated by the mixed boundary condition [34], and could be taken into account using an exploration distance C. We set the absorbing walls at $z=-C$ and $L+C$ to calculate the form factor, where $C=(2l^*/3)(1+\rho)/(1-\rho)$ is the exploration distance and ρ is the internal reflection coefficient. When the internal reflection can be ignored, the exploration distance can be estimated as $C=0.701l^*$ [33,34]. We replace $\langle \Sigma |W_\xi(r_s;R)|^2 \rangle$ in Eq. (5) with an integration over the distribution function of the trajectory, $\int ds P(r_s;R,s)$,

$$P(r_s;R,s)=\int dr'\int ds' G_0(r_s-r',s-s')\,\delta(s')\,\delta(R'-R)$$
$$\times\sum_n\,[\,\delta(z'-[2n(L+2C)+l^*])$$
$$-\delta(z'+[2n(L+2C)+l^*+2C])], \qquad (6)$$

where s is the path length of the trajectory, $r^2=R^2+z^2$, and $G_0(r,s)=\exp[-cr^2/4Ds]$ is the Green function in an infinite medium. Substituting Eq. (6) into (5), we obtain

$$C(r_s,\Delta k)=\frac{\cosh[2\beta(L+C-z_s)]-1}{\cosh[2\beta(L+2C)]-1}, \qquad (7)$$

where $\beta=\sqrt{\Delta k^2+(1/L_a)^2}$, $\Delta k=(2\pi/\lambda)\theta$, $L_a=\sqrt{l^* l_a/3}$ and l_a is the absorption length for the excitation light. The intensity propagator for the SH light $T_{SH}(R_d;r_s)$ is also calculated on the basis of diffusion approximation as

$$\int dR_d T_{SH}(R_d;r_s)=\frac{(z_1+C)(L+C-z_2)}{L+2C}, \qquad (8)$$

where $z_1=z_s, z_2=z_d=L-l^*$ for the transmission geometry and $z_1=z_d=l^*, z_2=z_s$ for the reflection geometry, respectively. The procedure to calculate the form factor is straightforward and similar to that used in the calculation of the persistent hole burning in Ref. [35]. Substituting Eqs. (7) and (8) into Eq. (2), we obtain the form factors for the transmission and the refection geometries as

$$I_{SH_T}(\beta)=\{4\beta^2\sinh^2[\beta(L+C)](L+2C)\}^{-1}$$
$$\times\{\cosh[2\beta(L+C)]+2\beta C\sinh[2\beta(L+C)]$$
$$-\cosh[2\beta C]-2\beta(L+C)\sinh[2\beta C]$$
$$-2\beta^2 L(L+2C)\} \qquad (9)$$

and

$$I_{SH_R}(\beta)=\{4\beta^2\sinh^2[\beta(L+C)](L+2C)\}^{-1}$$
$$\times\{-\cosh[2\beta(L+C)]+2\beta(L+C)$$
$$\times\sinh[2\beta(L+C)]+\cosh[2\beta C]$$
$$-2\beta C\sinh[2\beta C]-2\beta^2 L(L+2C)\}, \qquad (10)$$

respectively. The form factors of Eqs. (9) and (10) are similar to those in Ref. [19], in which real speckle fluctuations in SH light outside the medium were observed and the traditional procedure of the speckle measurement was performed. In contrast to Ref. [19] in the present situation no real speckle pattern is recorded, while speckle correlation is directly measured inside the medium through the nonlinear signal. The propagator $T_{SH}(R_d,r_s)$ as well as the order of the electric fields in the correlation function are different from the traditional measurement, which results in the different form factors. The theoretical results are summarized in Fig. 2(a). The width of the central peak is of the order of λ/L, where λ is the wavelength of the excitation light and the peak reflects the leading term of the correlations in the speckle fluctuations. The ratio of the correlation peak to the background is $C(\theta=0):C(\theta=\infty)=6:4$. Rapidly oscillating fringes are observed in the region of $\theta\lesssim\lambda/w$, where w is the beam size of the excitation beam.

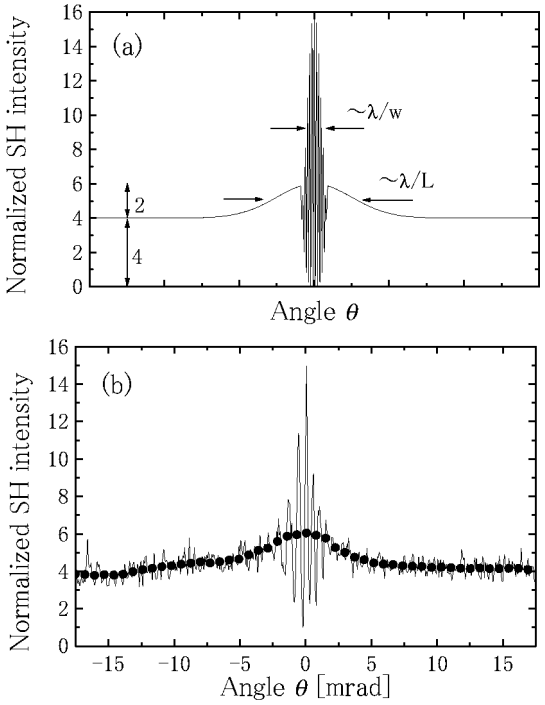

FIG. 2. (a) Schematic illustration of the total SH intensity as a function of the angle between two beams. (b) Experimental result of the total SH intensity in the transmission geometry. The solid line is the raw experimental datum and the solid circles are the results where the rapidly oscillating fringes were numerically averaged out.

III. EXPERIMENTS

We experimentally examined the total SH intensity generated in a disordered medium by angular correlated two excitation beams. The experimental setup is schematically illustrated in Fig. 3. The excitation light source was the fundamental light from a mode-locked Nd^{3+} yttrium-aluminum-garnet (YAG) laser. The pulse duration was 93 psec, the wavelength was 1064 nm, and the repetition rate was 82 MHz. Corpuscles of $LiNbO_3$ of about 3 μm in diameter were compacted between two optical glass plates and used as the sample. The transport mean free path was estimated as $l^*=7$ μm at 1064 nm by a total transmission experiment. The excitation beam was divided into two beams of equal pulse energy by a beam splitter. The average power of the excitation beam was 50 mW. Two beams were reflected by corner cube prisms and combined by the same beam splitter into parallel beams. These beams were focused onto the sample by a lens to make an angle θ with respect to each other. We changed the angle θ by translating CC1 (corner cure prism). In the reflection geometry experiments, the SH light (0.53 μm) from the incoming surface of the sample was collected by the same lens and led to a photomultiplier tube by dichroic mirrors M1 and M2. For the transmission

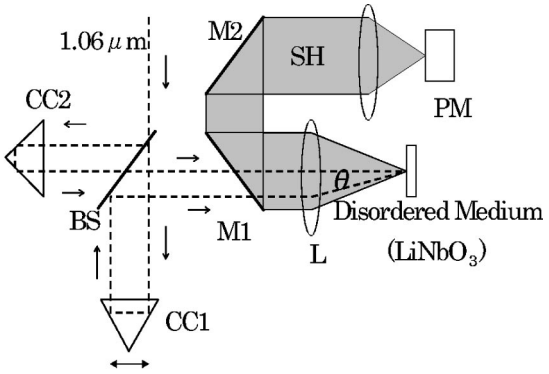

FIG. 3. Experimental setup in the reflection geometry. 1.06 μm represents the fundamental beam from the Nd^{3+} YAG laser; BS is the beam splitter; CC1 and CC2 are the corner cube prisms; L is the lens, M1 and M2 are the dichroic mirrors; SH represents the second-harmonics light generated in the disordered medium; PM is the photomultiplier tube.

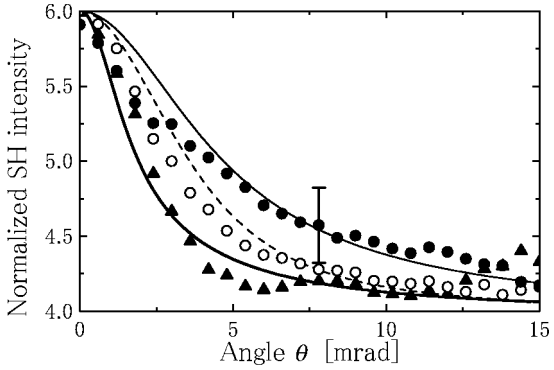

FIG. 4. Experimental results and theoretical curves for the total SH intensity. Solid circles and triangles are the experimental results in the reflection geometry for the samples of 97 μm and 270 μm thickness, respectively. Open circles are that in the transmission geometry for the sample of 97 μm thickness. Solid and dotted lines are the theoretical curves.

geometry experiment (not shown), the SH light was collected from the opposite side surface of the sample. It is noted that in the present experiment no real speckle pattern was recorded.

Figure 2(b) shows an experimental result of the SH intensity as a function of the angle θ. The sample thickness was 97 μm. The signal intensity was normalized so that the background is 4. The experimental result shown in Fig. 2(b) recaptures the theoretical prediction of Fig. 2(a). We see rapidly oscillating fringes in the $\theta\sim0$ region, and after these fringes tails of the correlation peak in both sides as a function of θ. When the angle between two beams is $\theta\sim0$, the volume speckle patterns generated by the two beams constructively interfere and the total SH intensity could increase. As the angle is increased, the SH intensity decreases to the level of ~4, which reflects the loss of the mutual correlation between two speckle patterns.

The dependence of the angular correlation peak on the sample thickness and the experimental geometry are shown in Fig. 4. The solid circles and triangles are the experimental data for the samples of 97 μm and 270 μm thickness, respectively, in the reflection geometry. The open circles are the data for the sample of 97 μm thickness in the transmission geometry. In this figure, rapidly oscillating fringes were numerically averaged out. We calculated the angular correlated SH intensity on the basis of Eqs. (9) and (10). With the refractive index $n=2.1$ of $LiNbO_3$ and the volume fraction 0.6, the internal reflection can be estimated as $\rho=0.38$ on the basis of the Fresnel's law [33]. The absorption both for the fundamental light and for the SH light is negligible in $LiNbO_3$, and we set as $L_a=\infty$. The thin and thick solid lines in Fig. 4 are calculated curves in the reflection geometry for the samples of 97 μm and 270 μm thickness, respectively. The broken line is that for the sample of 97 μm in the transmission geometry. The angular width of the correlation peak in the thick sample is narrower than that in the thin sample. Similarly, the correlation peak in the transmission geometry is narrower than that in the reflection geometry for the same sample.

In order to see characteristics of the present experiment in comparison with the traditional speckle measurements, we plotted the width of the correlation peak as a function of sample thickness L. Figure 5(a) represents the width of the peak in the present two beam correlation measurement calculated on the basis of the form factors of Eqs. (9) and (10). For comparison, we also plotted the width of the correlation function expected in the traditional speckle measurements, where real speckle patterns are observed outside the medium. For this purpose, the correlation function was evaluated from $C(r_s,\Delta k)$ in Eq. (7), assuming that r_s is located as $z_s=L-l^*$ and $z_s=l^*$ for the transmission and the reflection geometry, respectively. The form factor of Eq. (10) scales with

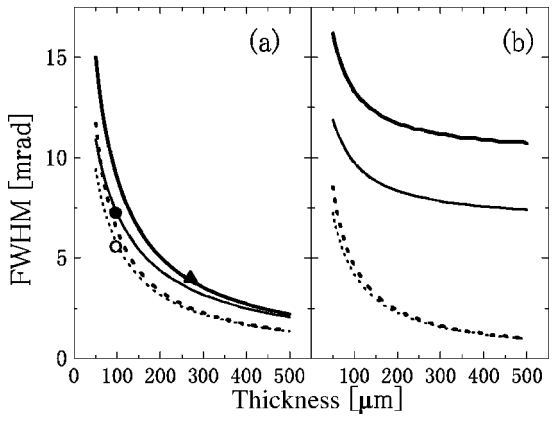

FIG. 5. (a) The width of the correlation peak as a function of sample thickness L. (b) The width of the correlation function expected in the traditional speckle measurement. Thick solid and thick dashed lines are calculated curves without the internal reflection in the transmission and the reflection geometries, respectively. Thin lines are the same but with the internal reflection $\rho=0.38$. In (a), solid and open circles represent the experimental data for the 97 μm sample in the transmission and reflection geometries, respectively. The solid triangle represents that for the 270 μm sample in the reflection geometry.

ΔkL rather than Δkl^* even in the reflection geometry. We also examined the effect of the internal reflection. The thin lines in Fig. 5 represent the width calculated in the case $\rho=0.38$, both for the present two beam correlation measurement and for the traditional measurements. In the traditional measurements, the effect of the internal reflection is strong in the reflection geometry, whereas it is weak in the transmission geometry [33]. On the other hand, the effect of the internal reflection is not significant even in the reflection geometry in the present measurement. In the present two beam correlation measurement, the SH light is generated at all place inside the sample. This SH light propagates through the sample, and appears both at the incoming and at the outgoing sample surfaces. This means that the signal observed in the reflection geometry still contains much information on the correlation function in the deep sample region. This mechanism explains why the form factor scales with ΔkL and the effect of the internal reflection is small even in the reflection geometry.

In the two beam correlation measurement, the width and shape of the correlation peak are also subject to the absorption either in the fundamental light or in the SH light. The form factors of Eqs. (9) and (10) are, however, essentially similar to that of the hole burning in a multiple scattering medium. In Ref. [35] we have calculated these effects. The absorption in the fundamental light broadens the correlation peak both in the transmission and in the reflection experiments. On the other hand the absorption in the SH light broadens the peak in the reflection experiment whereas makes the peak narrow in the transmission experiment.

The experimental data in Fig. 4 show a slight deviation from the calculated curves, specifically in the small angle region. We obtained these data by averaging the rapidly oscillating fringes. The discrepancy between the experiments and the calculations may appear because the number of the fringe is not enough. It is noted that in the present measurement, two excitation beams are injected simultaneously and the additional combinations of electric fields, which do not exist in the traditional speckle measurements, are possible. These terms generate rapidly oscillating fringes. Therefore, this is also the difference between the present and the traditional measurements.

Figure 6 shows the rapidly oscillating fringes at $\theta\sim 0$ observed with the excitation beams of different diameters. When the angle between two excitation beams is small, two fundamental beams interfere constructively or destructively and the total intensity of the excitation becomes 4 or 0, respectively. This situation continues as long as $\theta<\lambda/w$, and results in the rapidly oscillating fringes. We see that the width of the fringe envelope observed with the beam of $w=750\ \mu$m is narrower than that observed with $w=250\ \mu$m. The oscillation periods of fringes are not essential in this experiment. The fringes are subject to the phase difference between two beams. In our experiment, we made this phase difference by slightly rotating the translational axis of the stage of corner cube prism CC1.

In all the experiments discussed above, two beams were injected on the same spot of the sample. We also examined the SH intensity when the spatial overlap of two beams was dissolved under the condition $\theta\neq 0$. Figure 7 shows the experimental result on the SH intensity as a function of the beam separation distance d. The SH intensity at the beam separation $d\rightarrow\infty$ decreases from 4 to 2. This reflects that two of four base terms in Eq. (3), that is, $i=j=1$, $k=l=2$ term and $i=j=2$, $k=l=1$ term, vanish when the spatial overlap of two beams is dissolved.

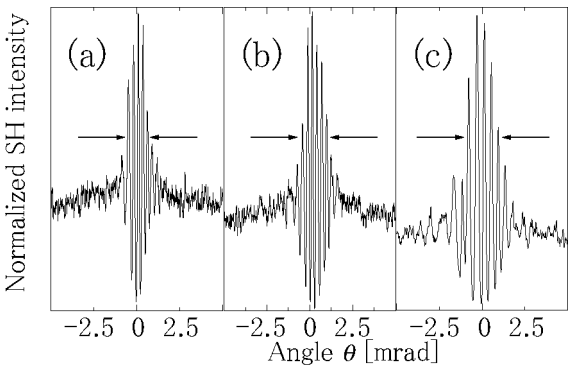

FIG. 6. Rapidly oscillating fringes at $\theta\sim 0$. The beam diameter is (a) $w=750\ \mu$m, (b) $w=500\ \mu$m, and (c) $w=250\ \mu$m. Arrows indicate the full width at half maximum of the fringe envelopes.

IV. DISCUSSION

The general agreements between the theory and the experiments verify that we can measure the speckle correlation in the disordered medium using two laser beams. The peak in Fig. 4 can be understood as the memory effect which has been investigated in the traditional speckle correlation experiments [13,14]. In contrast to the traditional speckle correlation experiments, the peak in Fig. 4 appears directly through the constructive interference of two volume speckle patterns produced by the two fundamental laser beams inside the medium.

An alternative way to explain the observation may be to consider the *macroscopic* interference fringe pattern produced by the two excitation beams. When the two beams make an angle θ, the interference effect produces a fringe pattern on the incoming surface of the sample as

$$I(R,z=0)=2E_0^2(1+\cos\Delta kR), \tag{11}$$

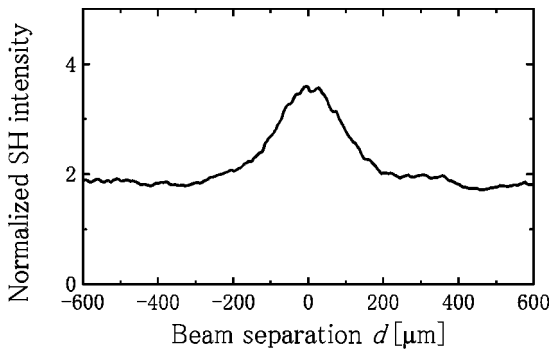

FIG. 7. Experimental result of the total SH intensity as a function of the beam separation distance d.

where E_0 is the electric field of the excitation beams. This interference pattern propagates diffusively through the sample thickness. We can calculate the interference pattern at z inside the medium using the diffusion equation as

$$I(R,z)=2E_0^2\left(1+\frac{\sinh[\Delta k(L-z)]}{\sinh[\Delta kL]}\cos\Delta kR\right). \quad (12)$$

The SH intensity generated inside the medium is proportional to the square of the local intensity of Eq. (12). Therefore, the SH intensity averaged over R is

$$I_{SH}(z)=\int dRI^2(R,z)=E_0^4\left(4+2\frac{\sinh^2[\Delta k(L-z)]}{\sinh^2[\Delta kL]}\right). \quad (13)$$

One may obtain the total SH intensity from the sample by integrating Eq. (13) over z. On the basis of Eq. (13), the angular correlation of the SH intensity can be understood as follows. When the angle between two excitation beams is small as $w^{-1}<\Delta k<L^{-1}$, the interference pattern propagates through the sample, keeping the high visibility. Since the SH intensity is proportional to the square of the local excitation intensity, this interference pattern, which produces bright and dark parts inside the medium, enhances the total SH intensity. As the angle is increased, the fringe period becomes short. When Δk becomes $\Delta k>L^{-1}$, the pattern is diffusively smeared and the SH intensity decreases. From Eq. (13), we can also see that the ratio of the base to the peak is 4:2, as is in Fig. 2. It should, however, be noted that the macroscopic interference patterns are carried by the microscopic speckle fluctuations. Therefore, the validity of the phenomenological treatment of Eq. (11) should be founded on the microscopic treatment of Eqs. (1)–(3). In addition, if we consider the higher order correlations, the macroscopic treatment may fail down, and we should directly start from Eq. (3).

V. CONCLUSION

We performed the two beam angular correlation experiment on the SH generation in the nonlinear disordered medium consisting of $LiNbO_3$ corpuscles. From this experiment, we could observe the speckle correlation inside the medium directly. In the present paper, we only dealt with the static disordered medium. If the medium is a dynamical system [36–38], such as aqueous suspensions of polystyrene latex, nonlinear signals from the sample could have information on the dynamics of the Brownian motion of scatterers. The two beam correlation measurement could also provide a method to examine dynamical characteristics of time dependent fluctuations.

[1] *Scattering and Localization of Classical Waves in Random Media*, edited by Ping Sheng (World Scientific, Singapore, 1984).
[2] M. P Van Albada and A. Lagendijk, Phys. Rev. Lett. **55**, 2692 (1985).
[3] P.E. Wolf and G. Maret, Phys. Rev. Lett. **55**, 2696 (1985).
[4] S. Etemad, R. Thompson, and M.J. Andrejco, Phys. Rev. Lett. **57**, 575 (1986).
[5] M. Kaveh, M. Rosenbluh, I. Edrei, and I. Freund, Phys. Rev. Lett. **57**, 2049 (1986).
[6] S. Etemad, R. Thompson, M.J. Andrejco, S. John, and F.C. MacKintosh, Phys. Rev. Lett. **59**, 1420 (1987).
[7] K.M. Yoo, S. Lee, Y. Takiguchi, and R.R. Alfano, Opt. Lett. **14**, 800 (1989).
[8] K. Totsuka and M. Tomita, Phys. Rev. B **59**, 11 139 (1999).
[9] H. Cao, Y.G. Zhao, S.T. Ho, E.W. Seelig, Q.H. Wang, and R.P.H. Chang, Phys. Rev. Lett. **82**, 2278 (1999).
[10] H. Cao, J.Y. Xu, S.-H. Chang, and S.T. Ho, Phys. Rev. E **61**, 1985 (2000).
[11] H. Cao, J.Y. Xu, D.Z. Zhang, S.-H. Chang, S.T. Ho, E.W. Seelig, X. Liu, and R.P.H. Chang, Phys. Rev. Lett. **84**, 5584 (2000).
[12] *Laser Speckle and Related Phenomena*, edited by J. C. Dainty (Springer-Verlag, Berlin, 1984).
[13] S. Feng, C. Kane, P.A. Lee, and A.D. Stone, Phys. Rev. Lett. **61**, 834 (1988).
[14] I. Freund, M. Rosenbluh, and S. Feng, Phys. Rev. Lett. **61**, 2328 (1988).
[15] R. Pnini and B. Shapiro, Phys. Rev. B **39**, 6986 (1989).
[16] M.P. van Albada, J.F. de Boer, and A. Lagendijk, Phys. Rev. Lett. **64**, 2787 (1996).
[17] A.Z. Genack, N. Garcia, and W. Polkosnik, Phys. Rev. Lett. **65**, 2129 (1996).
[18] J.F. de Boer, M.P. van Albada, and A. Lagendijk, Phys. Rev. B **45**, 658 (1992).
[19] J.F. de Boer, A. Lagendijk, R. Sprik, and S. Feng, Phys. Rev. Lett. **71**, 3947 (1993).
[20] *Analogies in Optics and Micro Electronics*, edited by W. van Haeringen and D. Lenstra (Kluwer Academic, Dordrecht, 1984).
[21] M. Tomita and T. Onimaru, J. Phys. Soc. Jpn. **65**, 3676 (1996).
[22] M. Tomita, Phys. Rev. B **45**, 1045 (1992).
[23] M. Tomita and K. Shimano, J. Phys. Soc. Jpn. **67**, 3761 (1998).
[24] V.E. Kravtsov, V.I. Yudson, and V.M. Agranovich, Phys. Rev. B **41**, 2794 (1990).
[25] A.R. McGurn, T.A. Leskova, and V.M. Agranovich, Phys. Rev. B **44**, 11 441 (1991).
[26] J. Martorell, R. Vilaseca, and R. Corbalan, Appl. Phys. Lett. **70**, 702 (1997).
[27] Y. Guo, P.P. Ho, H. Savage, D. Harris, P. Sacks, S. Schantz, F. Liu, N. Zhadin, and R.R. Alfano, Opt. Lett. **22**, 1323 (1997).
[28] J. Trull, J. Martorell, and R. Vilaseca, J. Opt. Soc. Am. B **15**, 2581 (1998).
[29] T. Ito and M. Tomita, Phys. Rev. E **63**, 036608 (2001).
[30] T. Ito and M. Tomita, J. Phys. Soc. Jpn. **70**, 2493 (2001).
[31] M. Tomita, in the Abstract of the Annual Meeting of Physical Society of Japan, 1998 (unpublished), p. 288.
[32] *The Quantum Theory of Light*, edited by R. Loudon (Oxford

University Press, Oxford, 1973).
[33] A. Lagendijk, R. Vreeker, and P. De Vries, Phys. Lett. A **136**, 81 (1989).
[34] J.X. Zhu, D.J. Pine, and D.A. Weitz, Phys. Rev. A **44**, 3948 (1991).
[35] M. Tomita, T. Ito, and S. Hattori, Phys. Rev. B **64**, 180202 (2001).
[36] G. Maret and P.E. Wolf, Z. Phys. B: Condens. Matter **65**, 409 (1987).
[37] D.J. Pine, D.A. Weitz, P.M. Chaikin, and E. Herbolzheimer, Phys. Rev. Lett. **60**, 1134 (1988).
[38] F.C. MacKintosh and S. John, Phys. Rev. B **40**, 2383 (1989).